Engineering Notes

ENGINEERING NOTES are short manuscripts describing new developments or important results of a preliminary nature. These Notes cannot exceed 6 manuscript pages and 3 figures; a page of text may be substituted for a figure and vice versa. After informal review by the editors, they may be published within a few months of the date of receipt. Style requirements are the same as for regular contributions (see inside back cover).

Study of Slat-Airfoil Combinations Using Computer Graphics

R. H. Liebeck* and D. N. Smyth*

Douglas Aircraft Company, McDonnell Douglas Corporation, Long Beach, Calif.

A SIMPLE theoretical model has been used with an "on-line" graphics program to study the basic effects of leading edge slat position and lift coefficient on the main airfoil pressure distribution and lift coefficient. The method, while providing an effective and efficient means for understanding the fundamental performance of a leading edge slat, has shown good agreement with an exact representation of the slat-airfoil combination.

The flow model used is that of a two-dimensional airfoil with a slat represented by a point vortex. Analytical solutions are obtained using conformal mapping of the flow about a circular cylinder and a point vortex, as shown in Fig. 1. The cylinder has circulation Γ_c and the point vortex has strength Γ_v. An image vortex of strength $-\Gamma_v$ is required to maintain the cylinder a streamline and an adjusting circulation Γ_A is needed to fix the rear stagnation point in order to satisfy the Kutta condition. A similar model was used by Neumark[1] to study rotating flaps, however, the present analysis accounts for the airfoil thickness and the interference effect between the slat (or flap) and the airfoil.

Analytical solutions of the airfoil alone have been long known and in the present study the unified approach of James[2] is used. The airfoil shape is generated by means of interior singularities or "poles," and the class of airfoils thus generated are designated "pole airfoils."

A particular airfoil is defined by selecting pole locations, orders, and strengths within the unit circle, e.g., the Joukowski airfoil is defined by a first-order pole plus a second-order pole located coincidently inside the circle.

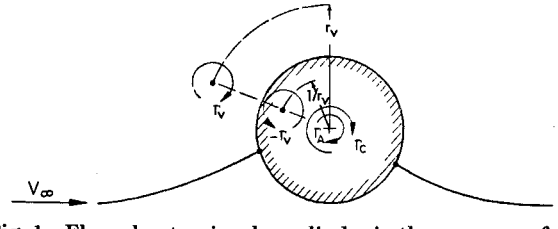

Fig. 1 Flow about a circular cylinder in the presence of an external point vortex. The rear stagnation point is fixed.

Presented as Paper 72-221 at the AIAA 10th Aerospace Sciences Meeting, San Diego, Calif., January 17-19, 1972; submitted February 3, 1972; revision received January 15, 1973. This work was performed under Contract F44620-70-C-0108 for the Air Force Office of Scientific Research, Washington, D.C. It is reported in more detail in Refs. 5 and 6.

Index categories: Airplane and Component Aerodynamics; Subsonic and Transonic Flow.

*Senior Engineer/Scientist, Aerodynamics Research Group. Member AIAA.

Altering their location and strength changes the camber and thickness of the resulting airfoil. A rigorous derivation and analysis of the pole airfoil theory together with the addition of the external point vortex is given in Ref. 2 and therefore only the application of this theory will be discussed here.

Since the entire flowfield about a pole airfoil plus point vortex can be described in closed analytic form, the study of this model lends itself particularly well to computer graphics. In this light, a computer program using the IBM System 360 computer together with the IBM 2250 display unit was written which provides "on-line" solutions. Operation of the program is basically as follows:

1) The strengths and locations of the poles which are to define the airfoil are specified in the circle plane as shown in Fig. 2. (The choice of the particular values used to obtain a desired shape is described in Ref. 2.) Figure 2 is a replica of the actual display which appears on the IBM 2250 screen. The pole specification values and the initial vortex location and strength are typed in on a keyboard.

2) Next, a transfer is made to the airfoil plane shown in Fig. 3 (which is also a picture of the actual IBM 2250 display). The top figure shows the airfoil geometry and location of the point vortex. The lower figures gives the airfoil surface velocity distribution as a function of s, the arc length along the airfoil surface beginning at the lower surface trailing edge. Three velocity distributions are shown: that for the airfoil alone, that imposed on the airfoil by the point vortex, and the combined result which represents the flow about the airfoil in the presence of the vortex. All of these solutions are exact.

3) The airfoil angle of attack and the vortex strength and location can be changed by merely keying in different values as desired. The results are immediately displayed on the IBM 2250 screen in the form of Fig. 3. At any time the display may be printed for later reference which is the source of Figs. 2 and 3.

4) The aerodynamic coefficients and parameters listed in Fig. 3 are defined and related as follows: a) ALPHA (α): Airfoil angle of attack as measured from the chord line. b) CL (C_L): Lift coefficient of the airfoil alone at that angle of attack. c) CL TOTL (C_{L_T}): Lift coefficient

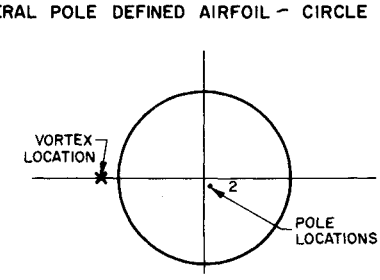

POLE DEFINITIONS

NO.	GRD	RADIUS	OMEGA	A	B
1	1	0.12	−50.0	1.0	0.0
2	2	0.12	−50.0	.0796	−.0777

VORTEX DEFINITIONS

	VALUE	DELTA
RADIUS	1.20	0.01
THETAV	180.0	0.0
DEL C_L	0.0	0.005

Fig. 2 Circle plane used for defining pole airfoil and initial point vortex location and strength.

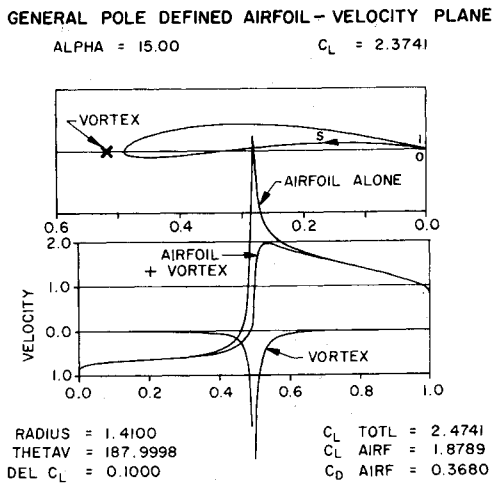

Fig. 3 Pole airfoil geometry and velocity distributions on airfoil alone and airfoil with vortex present. S is the arc length around the airfoil surface beginning at the lower surface trailing edge. The total airfoil perimeter equals one.

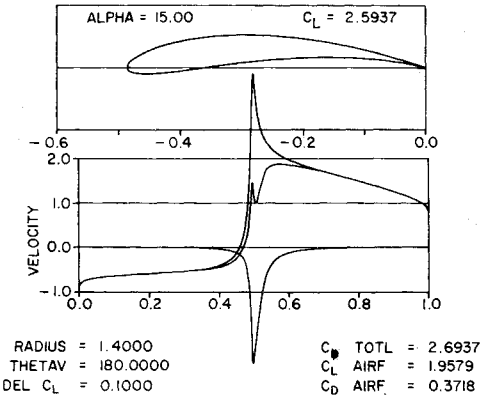

Fig. 4 Sample result showing spiked modulation distribution caused by the vortex being positioned incorrectly. Proper position is shown in Fig. 3.

of the total system (airfoil plus vortex). d) CL AIRF (C_{L_A}): Lift coefficient of the airfoil in the presence of the vortex. DEL CL (ΔC_L): Specified increment of lift for the total system (airfoil plus vortex) over the lift of the airfoil alone, i.e.,

$$C_{L_T} = C_L + \Delta C_L \tag{1}$$

e) CD AIRF (C_{D_A}): Drag coefficient of the airfoil in the presence of the vortex. (Drag on the vortex is equal and opposite to that of the airfoil.) f) RADIUS, THETAV (r_v, Θ_v): Location of the vortex in the circle plane. An effective "slat" lift coefficient is defined by

$$C_{L_S} = C_{L_T} - C_{L_A} \tag{2}$$

All of the aerodynamic coefficients are based on the airfoil chord and the freestream velocity, V_∞. This is more or less standard in multielement airfoil work, and allows convenient relations such as those given by Eqs. (1) and (2).

The various lifts coefficients are related by Eqs. (1) and (2), and typical operation of the program is as follows. Setting the airfoil angle-of-attack sets C_L, and setting ΔC_L specifies C_{L_T} from Eq. (1) or vice versa—independent of the position of the vortex so long as it lies outside of the airfoil. Moving the vortex will change C_{L_S} and C_{L_A} but they will always satisfy Eq. (2). The actual relation of these lift coefficients is derived from an application of Blasius' theorem to the two-body problem, and this is thoroughly described in Ref. 2.

It should also be noted that there is no net drag force on the airfoil plus vortex system as far as potential flow is concerned, and C_{D_A} represents a mutual repelling force between the vortex and the airfoil. It is this force which typically causes leading edge slats to extend automatically when released from their retracted position.

Figure 4 shows the result of an arbitrary specification of the vortex location and strength. It can be seen that this results in a severe and unwanted velocity spike near the leading edge. Leaving ΔC_L fixed and adjusting the vortex position yields a smooth modulated velocity similar to that shown in Fig. 3. It was found that it was quite easy to select the proper vortex location and strength in order to obtain a smooth velocity modulation. This represents one of the major features and justifications for employing the computer graphics capability. Some applications are now given.

Example 1

Here it is desired to increase C_{L_T} while holding $C_{P_{min}}$ on the airfoil to a specified value which might be set by separation criteria. First, the airfoil angle of attack was set so that $C_{P_{min}}$ reached the specified value with no vortex present. The angle of attack was then increased by a few degrees and the vortex strength and position adjusted so that $C_{P_{min}}$ was reduced to the specified value using the minimum possible vortex strength. This process was then repeated until the airfoil angle of attack reached 45° which is considerably beyond the range of practical operation. The resulting variations of the various lift coefficients are shown in Fig. 5 for a specified value of $C_{P_{min}} = -8$. Also shown is the implied slat chord C_S based on the ratio C_{L_S}/C_{L_T} which uses the crude approximation that the total lift is divided proportionally between the slat and airfoil chords.

Example 2

The purpose of this example was to test the validity of approximating a slat by a single point vortex. The geometry used was a 10% thick symmetrical Joukowski main airfoil with a cambered Joukowski airfoil whose chord was 10% of the main airfoil's for the slat. The slat was located in a typical position with respect to the main airfoil as shown in Fig. 6. The combination was then input into the Douglas Neumann potential flow program[3] at an angle of attack of 15° which provided the aerodynamic coefficients of the system and its elements together with the pressure distributions on the elements.

Next, using the pole-airfoil-plus-point-vortex program, a point vortex was located at the slat quarter chord point and ΔC_L was set so that the total load on the vortex ($C_{L_S}{}^2$

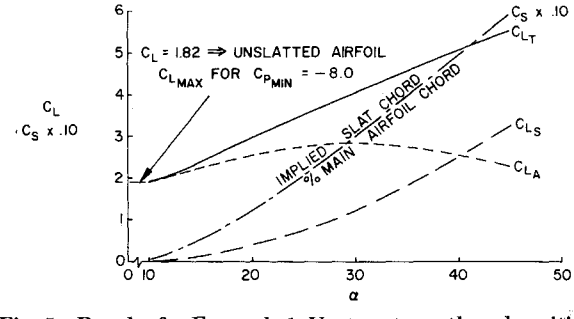

Fig. 5 Results for Example 1. Vortex strength and position adjusted to hole $C_{P_{min}} = -8.0$ constant as α is increased.

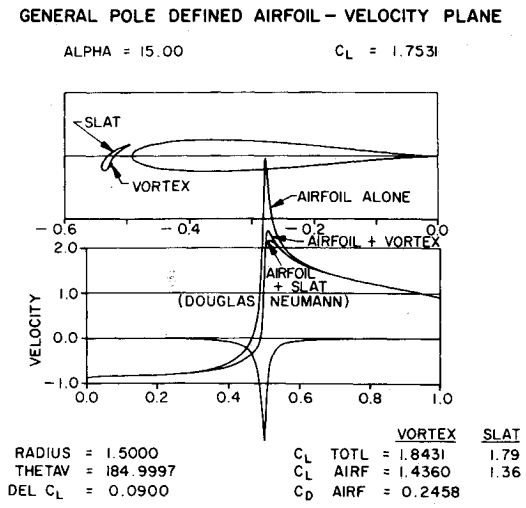

Fig. 6 Results for Example 2. Comparison of point vortex with a real slat using the Douglas Neumann potential flow program.

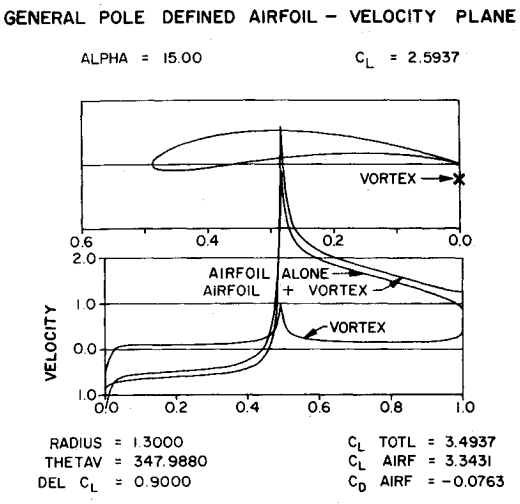

Fig. 7 Results for Example 3. Point vortex used to simulate a slotted flap.

+ $C_{D_A}{}^2)^{1/2}$ was equal to the total load on the slat as calculated from the Douglas Neumann program results. The resulting modulation distributions from both the point vortex and the slat are shown in Fig. 6, along with the values for C_{L_T} and C_{L_A}. The slat provides slightly more modulation than the vortex and thus the total lift of the slat plus airfoil system (C_{L_T} = 1.79) is less than that point vortex plus airfoil system (C_{L_T} = 1.84) for the same loading of the slat and point vortex.

Since the slat is positioned less than its chord length away from the nose of the airfoil, the above result is not surprising. It is expected that the distributed vorticity along the slat chord (as used in Ref. 4) would provide more effective modulation than the concentrated vorticity of the point vortex. However, these results do demonstrate that using a point vortex to represent a slat as a first-order theoretical model is a reasonable approach.

Example 3

The point vortex can also be used to simulate a slotted flap at the airfoil trailing edge. An example of this is shown in Fig. 7 where the vortex is located just below the trailing edge. The circulation about the flap (point vortex here) causes an acceleration of the flow near the trailing edge. However, this also increases the velocity peak at the leading edge as can be seen in Fig. 7 which calls for a leading edge slat (or, in the present context, a second point vortex). At this time, the pole-airfoil-plus-point-vortex program does not have the capability for generating two independent point vortices, but it appears that this would be a logical next step in developing the program.

References

[1]Neumark, S., "Rotating Airfoils and Flaps," *Journal of the Royal Aeronautical Society*, Vol. 67, Jan. 1963, pp. 47–63.

[2]James, R. M., "A General Class of Exact Airfoil Solutions," *Journal of Aircraft*, Vol. 9, No. 8, Aug. 1972, pp. 574–580.

[3]Hess, J. L. and Smith, A. M. O., "Calculation of Potential Flow About Arbitrary Bodies," *Progress in Aeronautical Sciences*, Vol. 8, edited by D. Kucheman, Pergamon Press, New York, 1966.

[4]O'Pray, J. E. and Lissaman, P. B. S., "Leading-Edge Slat Design by a Semi-Inverse Technique," *Journal of Aircraft*, Vol. 9, No. 2, Feb. 1972, pp. 143–149.

[5]Liebeck, R. H., "Theoretical Studies on the Aerodynamics of Slat-Airfoil Combinations," MDC J5195, May 1971, McDonnell Douglas Corp., Douglas Aircraft Co., Long Beach, Calif.

[6]Liebeck, R. H. and Smyth, D. N., "A Simple Model for the Theoretical Study of Slat-Airfoil Combinations," AIAA Paper 72-221, San Diego, Calif., 1972.

Errata

Application of Thermal Barriers to High-Temperature Engine Components

R. L. Newman, K. R. Cross, and W. C. Spicer
Detroit Diesel Allison Div., General Motors Corporation, Indianapolis, Ind.
and
H. D. Sheets and T. D. Driskell
Battelle Memorial Institute, Columbus, Ohio

[J. Aircraft, **9**, 609–610 (1972)]

The editors regret that the NTIS accession number of the full paper[1] was misprinted. It should read N72-24822.

Reference

[1]R. L. Newman, et. al., "Application of Thermal Barriers to High Temperature Engine Components," Paper 21-C-71F, American Ceramic Society, Ceramic-Metal Systems Div., Fall Meeting, St. Louis, Mo., Sept. 1971; also Detroit Diesel Allison Rept. RN-71-55, (Sept. 1971); also NTIS No. N72-24822.

Received March 9, 1973.
Index categories: Structural Composite Materials (Including Coatings); Thermal Modeling and Experimental Thermal Simulation.